Vol. 45, No. 1 (2023) 81-88, DOI: 10.24874/ti.1407.11.22.12

Tribology in Industry

www.tribology.rs

RESEARCH

Parametric Studies on Performance of Oil-Free Thrust Foil Bearings at Lower Speeds

S. Supreeth[a,*], T.N. Raju[a], R.N. Ravikumar[b], C.R. Mahesha[c]

[a]*Department of Mechanical Engineering, Dr. Ambedkar Institute of Technology, Bangalore – 560056, India,*
[b]*Department of Mechanical Engineering, BMS College of Engineering, Bangalore – 560019, India,*
[c]*Department of Industrial Engineering and Management, Dr. Ambedkar Institute of Technology, Bangalore – 560056, India.*

Keywords:

Thrust foil bearing
Load capability
Stiffness
Foils
Rotating speeds
Dimensionless Number

* Corresponding author:

S. Supreeth
E-mail: supreeth.s1994@gmail.com

Received: 25 November 2022
Revised: 6 December 2022
Accepted: 28 December 2022

A B S T R A C T

The present work involves an experimental analysis on gas-lubricated foil thrust bearing (FTB) that has major applications in food processing units at lower operating speeds. Parametric studies include testing thrust foil bearings with various foil configurations in terms of foil thickness, foil geometry, and foil material. Novel bearing testing apparatus designed and fabricated for the purpose supported a larger diameter (224 mm) thrust foil bearing, operated at speeds ranging from 10,000 rpm to 18,000 rpm. Performance of air foil thrust bearing (AFTB) concerning static structural stiffness and load bearing capability was determined in optimizing the best foil configuration. A novel dimensionless number was formulated that emphasizes the affecting factors of thrust foil bearing with respect to axial loads.

1. INTRODUCTION

A foil thrust bearing (FTB) is a self-acting hydrodynamic machine element that is capable of supporting rotating devices by a thin film of lubricating fluid (air) and hence they are termed as oil-free thrust foil bearing or gas-lubricated foil thrust bearing. The advantages of these bearings in turbo-machinery include reduced weight, removal of the conventional oil lubrication system, and synergistic use of working fluid. In these gas foil thrust bearings (GFTB), the converging wedge film developed between the foil and the runner forms a pressure profile which in turn supports the external thrust or axial loads. Experimental research on air foil thrust bearings (AFTB) was conducted earlier by Bauman [1] at NASA for a 100 mm bearing diameter at 80,000 rpm speeds. The performance of FTB in terms of coefficient of friction, load capacity, and temperatures was evaluated for grooved foils by Hyuga and others [2] for lower speeds. Similar performance tests were conducted on hydrodynamic gas foil journal bearing (GFJB) and foil thrust bearing (FTB) on a turbo-expander by T Lai et al. [3] for rotating speeds up to 52,000 rpm. Effect of foil stiffness and

nominal clearance on static performance of GFTB with top foil, bump foil, and supporting foil were tested for a centrifugal air compressors by Ting Shi and others [4]. Tae Ho Kim et al. [5,6] conducted parametric studies on dynamic characteristics of GFTB in terms of axial vibrational amplitude of the rotor at 20,000 rpm. Performance in terms of power was analyzed experimentally for a turbocharger supported by GFJB (as presented in ref. [7]) and GFTB for speeds catering up to 136,000 rpm by Y. B. Lee and others [8].

The effect of temperature on FTB with respect to operating speed and applied pre-load or static-load was determined by Liu and others [9] with a k-type thermocouple placed on top foils. Likewise the effect of pressurized cooling air at higher temperatures enhances the bearing axial loads as depicted by Yu Guo et al. [10] for higher speeds (up to 120,000 rpm) and ever before by Dykas and Prahl [11] for lower speeds (up to 55,000 rpm). A vertical bearing test rig developed by Kim and Park [12] examined the torque, temperature, and pressure on the GFTB for an applied static load at speeds ranging up to 25,000 rpm. Convex shaped wedge foil performed better as to concave and slope wedge foils in terms of load capacity as demonstrated by Hao Li et al. [13] for FTB operated at 96,000 rpm. Recent studies on multilayer FTB by Changlin and others [14] spotted that foil stiffness parameter play a major role in enhancing load capability of the bearing. Experimentations on GFTB were conducted by Ravikumar et al. [15,16] with only top foil for speeds up to 45,000 rpm using square foils, angular foils, and cascaded foils for inner edge of the foil being same and different with respect to outer edge. Supreeth and others [17] performed parametric analyses in optimization of foil stiffness for a GFTB of 60 mm diameter that included some CFD simulations. Also, reviews on AFTB [18,19] has enlightened on the factors affecting the performance of the bearing including some informative research gaps.

Oil-free bearings of larger diameter, operating at speeds catering up to 20,000 rpm are in great need for food processing industries while the current research addresses in realizing higher load carrying capacity of air foil thrust bearings at lower speeds (ranging between 10,000 rpm and 18,000 rpm). Besides mounting of foils being simple, the present design of FTB has a single layer of cantilevered leaf structured foil without any bump foil or viscoelastic support as in the case of typical foil bearings. As the foil stiffness plays a key role in bearing load, variation of stiffness of a single layer wedge-shaped foil was found sufficient in arriving at an optimized thrust loads. This in turn, eliminates the bumps or supports by reducing the overall mass and cost including the fabrication techniques with available foil material.

2. EXPERIMENTATION

An instrumental rig designed and fabricated for testing the thrust foil bearings is a standalone unit that consists of a power unit, drive unit, cooling unit, bearing unit, and loading unit. The experimental rig is sketched in figure 1 for better understanding and the test set-up is pictured in figure 2.

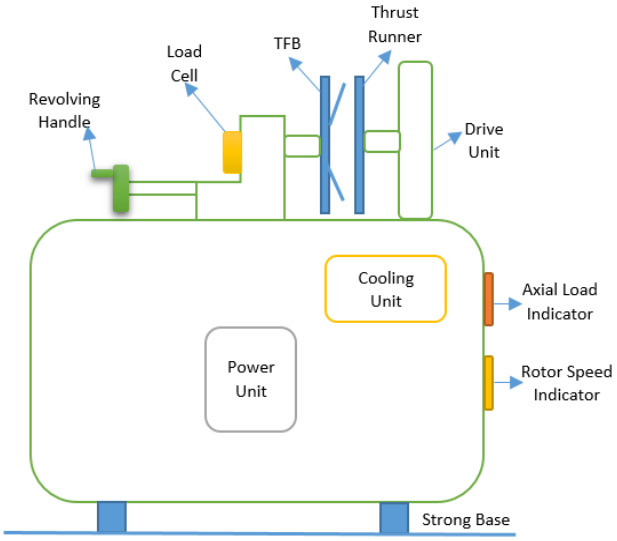

Fig. 1. Schematic diagram of the bearing test rig.

Fig. 2. Photograph of the GFTB test rig setup.

The thrust runner made up of aluminium alloy is mounted on a spindle rotated by a belt driven AC motor that requires a total power of 6 kW. The foil thrust bearing (FTB) assembly is mounted on a horizontal sliding pedestal along the axis of the runner with a movement by a rotating wheel arrangement as shown in figure 3.

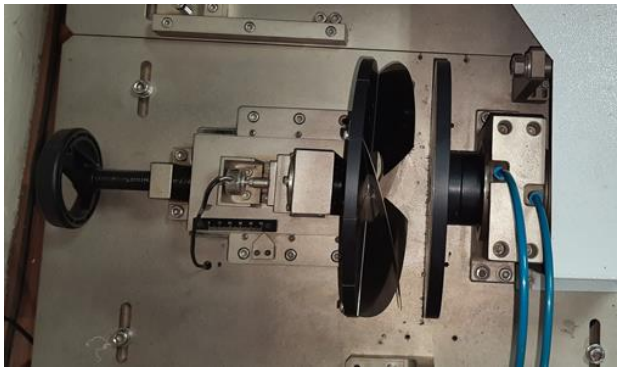

Fig. 3. Top view of the experimental rig.

The thrust force acting on this bearing pad with foils are measured by a load cell placed over the pedestal plate. The speed of the rotating disc or thrust runner is controlled by a variable-frequency drive (VFD) and is measured by means of a proximity sensor. The axial load in terms of N (newtons) and speed in terms of rpm (revolutions per minute) are displayed on the controller panel while the displacement of bearing assembly is measured by a scale on the sliding plate. To prevent the rise of temperature on the bearing at higher speeds, water cooling arrangement is provided to cool the rotating spindle. The cooling unit is filled with 3 litres of distilled water with a submersible pump that supplies water into the spindle housing while the used water flows back for recirculation.

The bearing pad or plate made with aluminium alloy consists of 12 circumferential slots with fixing holes for attachment of the angular foils (loading pads) with a maximum surface contact area of 36,191 mm^2 (which is more in comparison to previous research). The bearing pad with dimensions is shown in figure 4, while the drawing of 60° sector angled foil is illustrated in figure 5. Thin metallic foils of EC grade copper (Young's Modulus, E being 130,000 N/mm^2) and SS304 grade steel (with E = 193,000 N/mm^2) with thicknesses of 0.3 mm, 0.4 mm, and 0.5 mm are prepared for various sector angles (45°, 60°, 75°, and 90°). Laser cutting technology was employed in profile cutting where four pieces of leaf structured foils or pads were cut from sheets with 0.3 mm thickness for all sector angles. Similar cutting were employed with 0.4 mm and 0.5 mm thickened sheets for 45°, 60°, 75°, and 90° sector angles (SA). CNC metal press was used in bending the angular wedge foils which are mounted on the blackened bearing pad using fasteners for easy removal as depicted in figure 6. The foil inclination angle or the ramp angle is the wedge angle between the foil and the runner (or the bearing pad), is kept constant (α being 10°) for all the fabricated foils.

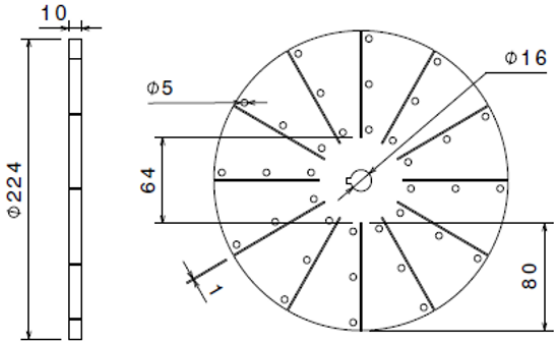

Fig. 4. Geometric drawing of the bearing pad.

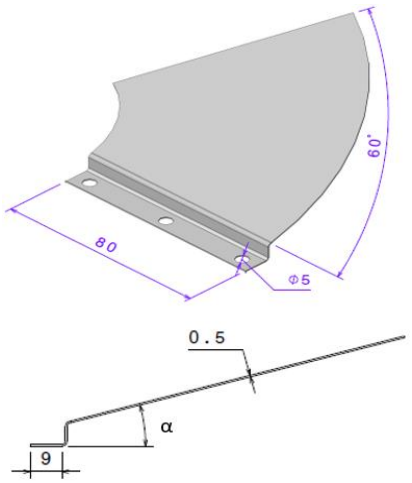

Fig. 5. Drawing of a 60° sector angular foil.

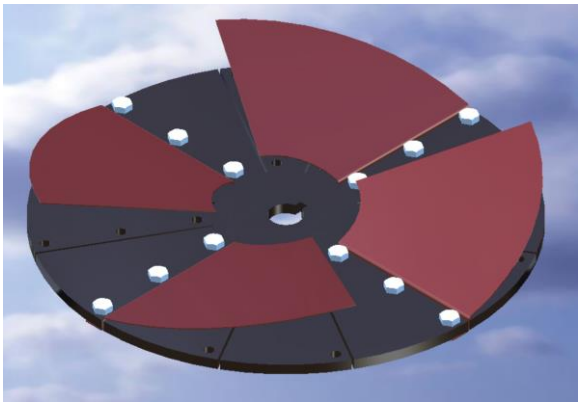

Fig. 6. Bearing assembly with 4 copper foils.

3. RESULTS AND DISCUSSIONS

Experimentations were conducted for all the combinations of thrust foil bearings (as indicated in table 1) on the test rig for both static and dynamic conditions. Although material property does not affect the load enhancement except the surface roughness, two easily available foil materials (steel and copper) are used in the present study. The thickness of the foil is mainly selected based on the diameter of the bearing and foil stiffness i.e., for large bearing diameter thicker foils are required to sustain axial loads with lesser deflections while higher stiffness are obtained with thicker foils for large cross sectional area of the AFTB. The investigative studies were conducted on FTB in terms of load carrying capabilities as a function of pre-load or the minimum distance between the runner and the bearing assembly which is an operational parameter. The experimental procedure and the results obtained for various FTB combinations at atmospheric conditions are discussed in detail.

3.1 Static tests

Four steel angular foils of 0.3 mm thickness with 45° sector angle (cleansed thoroughly for smooth surface) are attached on the backing plate with fasteners. This bearing assembly is mounted on the pedestal on the test rig with a keyway meanwhile the motion of the thrust foil bearing being restricted in all directions. The pedestal is manually moved with the help of revolving handle so that the all the foils of the bearing approaches towards the runner parallelly. However, the height of the inner edge (IE) and the outer edge (OE) of the foil are not same with respect to the bearing pad surface or the thrust runner (IE≠OE). Once the foils are in contact with the runner an axial load is induced which is indicated on the test rig digitally. The movement of the bearing assembly towards the thrust runner is continued until all the foils deflects with heights of IE and OE being same and parallel to the runner (i.e., IE=OE) with a maximum pre-load being applied. The distance between the thrust runner and the bearing assembly at this moment (which is about 5 mm), is almost same for the bearing assembly with all combination of foils while the applied pre-load being different for different sector angled foils. The deflection of the foils for pre-load are noted based on displacement of the pedestal movement by a measurement scale placed on the sliding bed of the test ring. This load-deflection ratio of all the foils yields static structural stiffness of the AFTB for 0.3 mm thickened steel foils with SA 45°.

Table 1. Parameters of the tested FTB.

Inner diamter of the foil, d_i	64 mm
Outer diamter of the foil, d_o	224 mm
Foil inclination angle, α	10°
Sector angles of the foil, θ	45°, 60°, 75°, and 90°
Foil thickness considered, t	0.3 mm, 0.4 mm, and 0.5 mm
Operating speeds, N	10 krpm, 12 krpm, 14 krpm, 16 krpm, and 18 krpm

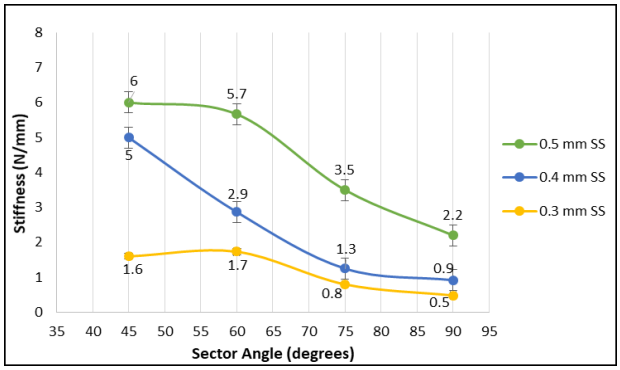

Fig. 7. Static structural stiffness of AFTB with steel foils.

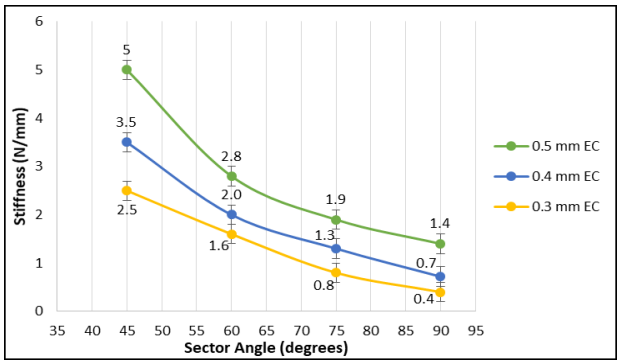

Fig. 8. Static structural stiffness of AFTB with copper foils.

The procedure is repeated by mounting and dismounting the FTB for all the other sector angles (60°, 75°, and 90°) of 0.3 mm steel foils. Each time the bearing assembly with required set of foils are fixed parallel to the thrust runner on the sliding pedestal for measurements. Similar static stiffness values of AFTB with 0.4 mm and 0.5 mm thickness steel angular foils of all sector angles are obtained experimentally and are plotted as shown in figure 7. From the values it is evident that the FTB with least sector angled foil (SA=45°) had higher stiffness compared to all three foil thicknesses tested and the thrust foil bearing

with 0.5 mm foil thickness had the highest possible stiffness of about 6 N/mm. Corresponding static results of AFTB with copper foils of 0.3 mm, 0.4 mm, and 0.5 mm thicknesses for all four sector angles are plotted in figure 8. From the graph the static structural stiffness is higher for the FTB with 45° sector angled copper foil with 0.5 mm thickness. Nevertheless the stiffness values of FTB with copper foils behaved similar to that of FTB with steel foils, the steel foils had higher stiffness to that of copper foils for a given or constant foil geometry.

3.2 Dynamic tests

Parametric experimentations were conducted for dynamic conditions with runner speeds catering between 10,000 rpm and 18,000 rpm for all the foil combinations of FTB. The bearing assembly with four sets of steel foils of 0.3 mm thickness with 45° SA mounted on opposite sides with maximum pre-load being applied and with IE=OE is maintained as in static case. The thrust runner is rotated anti-clockwise direction by regulating the VFD control for speeds up to 10,000 rpm. Initially the foils makes contact (rub) with the runner surface till the rotor reaches higher speeds meanwhile all the foils deflects due to pressurised air that carries the thrust load by forming a wedge film region, which is visible when viewed tangentially. The thrust load is now noted from the test rig for respective rotating speeds while this dynamic load is the maximum axial force acting on all the foils due to the fluid (air) pressure that deflects the foils forming a fluid film or air gap. Similar load readings were recorded for the FTB at 12,000 rpm, 14,000 rpm, 16,000 rpm and 18,000 rpm speeds. The wear on the foil surface due to the rubbing action with thrust runner until the lift-off speed (around 5000 rpm) is usual for all foils combinations of FTB at dynamic condition.

This experimental procedure is repeated for AFTB with other three sector angles (60°, 75°, and 90°) of steel foils with 0.3 mm foil thickness and the values are plotted in figure 9. From the graph it is evident that GFTB with 60° SA foil supported higher loads than that of 45° SA, while 75° and 90° SA foils carried lower thrust loads as the stiffness of these foils are less due to larger sector angles. The load capability of these bearings increased at higher rotating speeds (not linear though) with each configuration of foils having its own peak load bearing capacity concerning to different operating speeds i.e., at greater speeds the foils deflects soon that loses its stiffness by carrying lesser loads. It can be seen from the plots that AFTB with 90° SA foils had peak load at 14,000 rpm to 16,000 rpm speeds and at 18,000 rpm the foils deflected more with lesser load bearing capability.

Similar parametric studies on AFTB with speeds ranging from 10,000 rpm to 18,000 rpm for 0.4 mm thickness steel foils for all sector angles are plotted in Figure 10. It is observed that FTB with 0.3 mm steel foils with 60° sector foils carried higher loads due to large foil wedge area, while the FTB with 0.4 mm thickness steel foils of 45° sector angle supported higher loads, due to higher foil stiffness with lesser sector angle. Furthermore, values of the thrust foil bearing with 0.4 mm thickness of steel foils depicted a load increment of nearly two times with that of 0.3 mm foil thickness and hence geometrical stiffness played a major role in enhancing the axial loads. Experiments for AFTB mounted with copper foils of 0.3 mm and 0.4 mm foil thickness for all four sector angles are plotted in figure 11 and 12 respectively and the curves obtained were similar to that of steel foils. Results from dynamic tests for all foil configurations depicted that steel foils of 45° SA with 0.4 mm thickness carried thrust loads up to 42 N at 18,000 rpm.

Although sincere efforts were made in testing the thrust foil bearing with steel and copper foils of 0.5 mm thickness, no load could be drawn either due to the low operating speeds (air pressure) that were not enough in deflecting the foils or due to stiffness of the foil being high based on increase in foil thickness. It was observed that the load carrying capacity of the bearing increases by increasing the rotating speeds, likewise the increase in foil thickness of the AFTB. However, the thrust load of an AFTB is highest for an optimum foil stiffness (in terms of foil geometry), foil thickness, and operating speeds. From these graphs it is evident that the sector angle also has a vital role in load carrying capability concerning to various foil thicknesses. The thrust foil bearing assembly with 60° steel and 45° copper foils after dynamic tests are presented in figure 13 that pictures slight wear on the foil surface due to start and stop cycles.

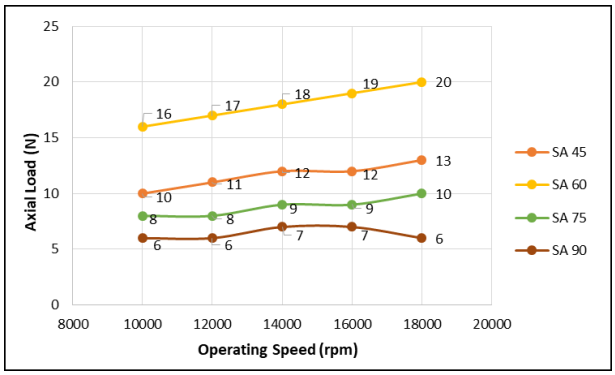

Fig. 9. Dynamic test results of GFTB with steel foils of 0.3 mm thickness.

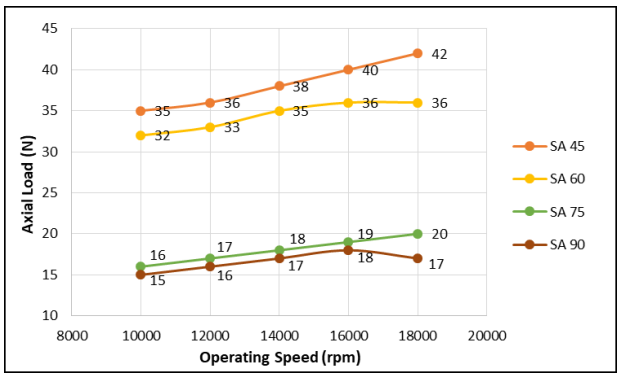

Fig. 10. Dynamic test results of GFTB with steel foils of 0.4 mm thickness.

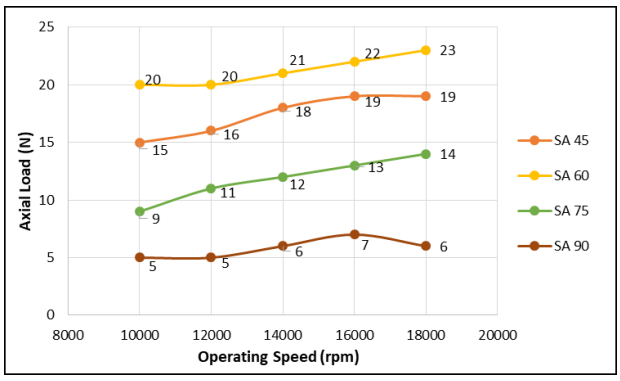

Fig. 11. Load capacity of GFTB with copper foils of 0.3 mm thickness.

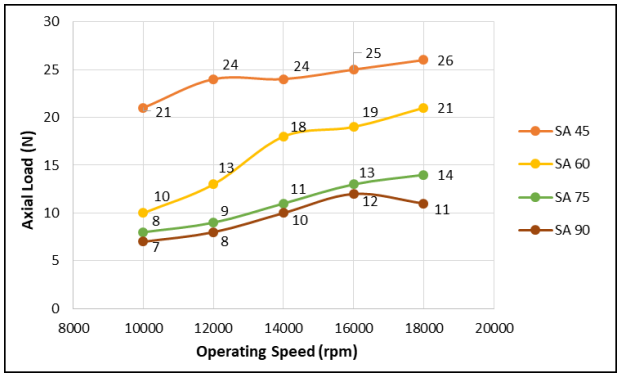

Fig. 12. Load capacity of GFTB with copper foils of 0.4 mm thickness.

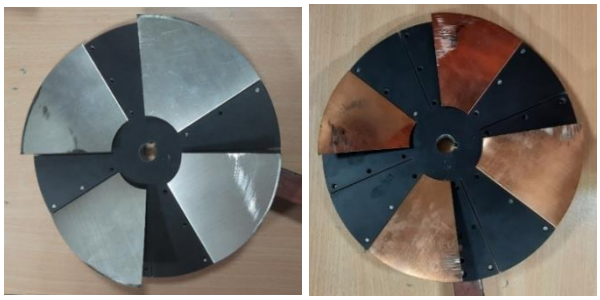

Fig. 13. Photographs of post-tested FTB with 60° steel and 45° copper foils.

The numerical values of static and dynamic tests presented in all graphs are the average of three experimental trials conducted for all the configuration of thrust foil bearings. Careful observations were made in recording down the values from the test rig that was calibrated before and after conducting experiments.

3.3 Bearing dimensionless number

A novel non-dimension number termed as bearing dimensionless number (BDN) was formed with all the load affecting parameters of the thrust foil bearing. The number holds good not only for the bearing with top foil (present work) but also for AFTB with bump foils or viscoelastic supports as foil stiffness plays a major role in terms of load bearing capability. The main factors included in formulating the BDN are foil static stiffness, foil geometry including foil thickness and foil material property as they form the significant stiffness characteristics of GFTB. The BDN in terms of equation is presented as below:

$$\mathrm{BDN} = \left\{\frac{\theta}{\alpha}\left(\frac{\mathrm{Do}-\mathrm{Di}}{\mathrm{Di}}\right)\left(\frac{\mathrm{E}\cdot\mathrm{t}}{\mathrm{k}}\right)\right\} \quad (1)$$

where, θ denoting the sector angle (SA) of the foil (in radians), α denoting the inclination angle (IA) of the foil (in radians), D_o representing the outer diameter of the foil (mm), D_i representing the inner diameter of the foil (mm), E being the young's modulus of the foil material (N/mm^2), t being the foil thickness (mm), and k being the static stiffness of all foils (N/mm) of AFTB.

The thrust load of the AFTB at dynamic condition is directly proportional to θ, α, E, t, k, and bearing contact surface area (Do-Di/Di) nevertheless up to an optimum condition. The BDN for all the varying parameters of the foil bearing configurations are calculated (however α, Do, and

Di are constant in present work) and are plotted against the thrust loads obtained from the dynamic tests for both the foil materials. Graphical points from figure 14 depicts the axial load capability of an AFTB is higher for lowest BDN, while the thrust foil bearing with higher BDN supported lesser loads. BDN for a particular FTB carries higher loads at higher operating speeds which is evident from the plot, while the FTB that supported constant loads at varying speeds have similar (merged) points as seen from the graph. Although BDN signifies the performance of GFTB in terms of load bearing capability, the bearing number holds good for a particular range of static stiffness and foil geometry for which the dynamic experimental results would be obtained.

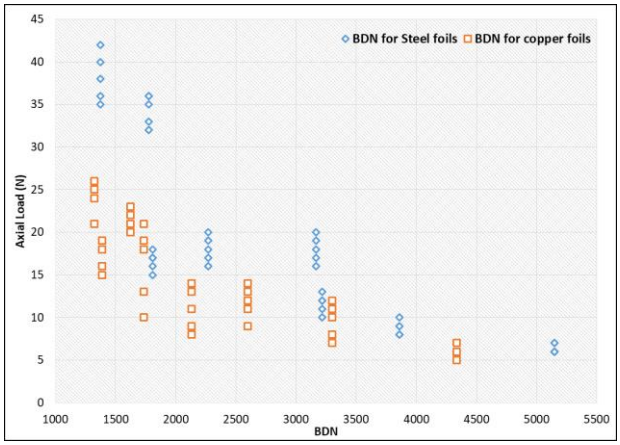

Fig. 14. BDN for various configurations of AFTB.

4. CONCLUSIONS

Parametric studies on gas lubricated thrust foil bearings with numerous foil configurations were tested for static and dynamic conditions on a newly developed instrumented bearing testing rig. Experimental results obtained for various operating speeds are plotted in optimizing a finest AFTB that supports larger axial loads. Major inferences drawn from the present experimental research include the following:

- The static structural stiffness of the FTB mainly depends on the foil stiffness in terms of foil geometry and foil thickness.
- The dynamic thrust load of the FTB is higher at greater operating speeds with increase in foil thickness for both steel and copper foils, however up to an optimum level.
- Both foil materials supported higher thrust loads for lower sector angled foil with larger wedge surface area at all rotating speeds.
- Each GFTB exhibited its own peak thrust load with different foil combinations concerning to foil thickness, foil sector angle, and foil material for a set of operating parameters.
- The calculation of BDN and its validation signifies the performance of AFTB in connection with load bearing capabilities for a wide range of parameters.

Acknowledgements

The authors are grateful to DRDO / GTRE (Ref. no. GTRE/GATET/CS36/1617/116/16/01) for their funding in procurement of the bearing testing rig and VGST / KSTePS (GRD no. 926) a CESEM research grant by Government of Karnataka, towards their financial assistance in recurring expenditure of the research project. In addition to this, the authors owe their gratitude to Dr. V. Arunkumar, Rtd. Scientist and Head, Propulsion Division, CSIR-NAL, Bangalore, India, for his research ideas and technical suggestions and also Research & Development Laboratory, Department of Mechanical Engineering, Dr. Ambedkar Institute of Technology, Bangalore, India, for their support in carrying out the present work.

REFERENCES

[1] S. Bauman, *An Oil-Free Thrust Foil Bearing Facility Design, Calibration, and Operation*, NASA Technical Reports Server, 2005.

[2] H. Kikuchi, M.D. Ibrahim, M. Ochiai, *Evaluation of Lubrication Performance of Foil Bearings with New Texturing*, Tribology Online, vol. 14, iss. 5, pp. 339–344, 2019, doi: 10.2474/trol.14.339

[3] T. Lai, Y. Guo, W. Wang, Y. Wang, Y. Hou, *Development and Application of Integrated Aerodynamic Protuberant Foil Journal and Thrust Bearing in Turboexpander*, International Journal of Rotating Machinery, vol. 2017, pp. 1-13, 2017, doi: 10.1155/2017/8430943

[4] T. Shi, H. Huang, Q. Chen, X. Peng, J. Feng, *Performance investigation and feasibility study of novel gas foil thrust bearing for hydrogen fuel cell vehicles,* International Journal of Energy Research, vol. 46, iss. 9, pp. 12642–12659, 2022, doi: 10.1002/er.8033

[5] T.H. Kim, M.S. Park, J. Lee, Y.M. Kim, K.-K. Ha, J. Park, C. Lee, C. Kim, *Identification of Dynamic Characteristics of Gas Foil Thrust Bearings Using Base Excitation*, in Proceedings of ASME Turbo Expo 2016 Turbomachinery Technical Conference and Exposition, 13-17 June, 2016, Seoul, South Korea, pp. 1–10, doi: 10.1115/GT2016-56282

[6] T.H. Kim, Y.B. Lee, T.Y. Kim, K.H. Jeong, *Rotordynamic performance of an oil-free turbo blower focusing on load capacity of gas foil thrust bearings,* Journal of Engineering for Gas Turbines and Power, vol. 134, iss. 2, pp. 1–7, 2012, doi: 10.1115/1.4004143

[7] V. Mouryaa, S.P. Bhoreb, *Investigation and Optimization for Performance Characteristics of Bump-type Foil Journal Bearings with Various Foil Materials*, Tribology in Industry, vol. 44, no. 4, pp. 664-686, 2022, doi: 10.24874/ti.1334.07.22.11

[8] Y.B. Lee, D.J. Park, T.H. Kim, K. Sim, *Development and performance measurement of oil-free turbocharger supported on gas foil bearings*, Journal of Engineering for Gas Turbines and Power, vol. 134, iss. 3, pp. 1–7, 2012, doi: 10.1115/1.4004719

[9] X. Liu, C. Li, J. Du, G. Nan, *Thermal Characteristics Study of the Bump Foil Thrust Gas Bearing*, Applied Sciences, vol. 11, iss. 9, pp. 1-19, 2021 doi: 10.3390/app11094311

[10] Y. Guo, Y. Hou, Q. Zhao, X. Ren, S. Chen, T. Lai, *Numerical and experimental studies on the thermal and static characteristics of multi-leaf foil thrust bearing,* Proceedings of the Institution of Mechanical Engineers, Part J: Journal of Engineering Tribology, vol. 236, iss. 3, pp. 1-16, 2021, doi: 10.1177/13506501211011019

[11] B. Dykas, J. Prahl, C. DellaCorte, R. Bruckner, *Thermal management phenomena in foil gas thrust bearings*, in Proceedings of ASME Turbo Expo 2006, Power for Land, Sea, and Air, vol. 5, 8-11 May, 2006, Barcelona, Spain, pp. 1417–1423, doi: 10.1115/GT2006-91268

[12] C.H. Kim, J. Park, *Testing of Load Capacity of a Foil Thrust Bearing,* Tribology and Lubricants, vol. 34, iss. 6, pp. 300–306, 2018, doi: /10.9725/kts.2018.34.6.300

[13] H. Li, H. Geng, L. Qi, L. Gan, *Effects of wedge curvature on performances of foil thrust bearing and the profile design in compressor system,* Proceedings of the Institution of Mechanical Engineers, Part J: Journal of Engineering Tribology, vol. 235, iss. 9, pp. 1-11, 2020, doi: 10.1177/1350650120975524

[14] C. Li, J. Du, J. Li, Z. Xu, C. Zhao, *Investigations on the Load Capacity of Multilayer Foil Thrust Bearing Based on an Updated Complete Model,* Journal of Tribology, vol. 145, iss. 2, pp. 1–18, 2022, doi: 10.1115/1.4055130

[15] R.N. Ravikumar, K.J. Rathanraj, V. Arun Kumar, *Experimental Studies on Air Foil Thrust Bearing Load Capabilities Considering the Effect of Foil Configuration*, Applied Mechanics and Materials, vol. 813–814, pp. 1007–1011, 2015, doi: 10.4028/www.scientific.net/AMM.813-814.1007

[16] R.N. Ravikumar, K.J. Rathanraj, V.A. Kumar, *Comparative Experimental Analysis of Load Carrying Capability of Air Foil Thrust Bearing for Different Configuration of Foil Assembly,* Procedia Technology, vol. 25, pp. 1096–1105, 2016, doi: 10.1016/j.protcy.2016.08.215

[17] S. Supreeth, R.N. Ravikumar, T.N. Raju, K. Dharshan, *Foil stiffness optimization of a gas lubricated thrust foil bearing in enhancing load carrying capability,* Materials Today: Proceedings, vol. 52, pp. 1479–1487, 2022, doi: 10.1016/j.matpr.2021.11.210

[18] K.J. Rathanraj, R.N. Ravikumar, *A Research trends in Air foil thrust bearings used in micro turbines and aircraft machines*, International Journal of Emerging trends in Engineering and Development, vol. 2, iss. 1, pp. 13–24, 2016.

[19] S. Shivakumar, T. NagaRaju, R.N. Ravikumar, M.C. Rudraiah, *A Review on Performance Characteristics of an Air Foil Thrust Bearing,* Tribology Online, vol. 17, iss. 4, pp. 276–282, 2022, doi: 10.2474/trol.17.276